catalysts

MDPI

Article

Continuous Dimethyl Carbonate Synthesis from CO_2 and Methanol Using Cu-Ni@VSiO as Catalyst Synthesized by a Novel Sulfuration Method

Meng Zhang [1,2,†], Kirill A. Alferov [1,2,†], Min Xiao [1], Dongmei Han [1], Shuanjin Wang [1,*] and Yuezhong Meng [1,*]

1 The Key Laboratory of Low-Carbon Chemistry & Energy Conservation of Guangdong Province/State Key Laboratory of Optoelectronic Materials and Technologies, Sun Yat-sen University, Guangzhou 510275, China; zhangmeng@smu.edu.cn (M.Z.); kirill-alpherov@yandex.ru (K.A.A.); stsxm@mail.sysu.edu.cn (M.X.); handongm@mail.sysu.edu.cn (D.H.)

2 School of Biomedical Engineering, Southern Medical University, Guangzhou 510515, China

* Correspondence: wangshj@mail.sysu.edu.cn (S.W.); mengyzh@mail.sysu.edu.cn (Y.M.); Tel.: +86-020-841-14113 (Y.M.)

† Meng Zhang and Kirill A. Alferov have contributed equally to this work.

Received: 23 January 2018; Accepted: 29 March 2018; Published: 3 April 2018

Abstract: Conversion of carbon dioxide into useful chemicals is a valuable task. One way to perform it is to transform CO_2 into dimethyl carbonate (DMC) by a reaction with methanol. Catalyst exerts significant impact on this process. During this work, Cu-Ni@VSiO bimetallic catalysts were successfully synthesized by traditional solution and novel sulfuration methods. The catalytic materials were characterized by several analytical techniques and were tested in a continuous fixed-bed reactor under different reaction conditions to promote DMC synthesis from CO_2 and methanol in the absence of dehydrating agents. The effects of reaction temperature, pressure, space velocity, metal loading, and bulk density on the catalytic performance were investigated in detail. It was found that the activity of Cu-Ni@VSiO catalyst with the support obtained by the novel sulfuration method is about three times higher when compared to that of the catalyst with the support that is synthesized by the traditional solution method. This result may stem from the difference in microstructure of the studied catalytic materials.

Keywords: copper-nickel catalysts; dimethyl carbonate; carbon dioxide; fixed bed reactor

1. Introduction

Dimethyl carbonate is one of the promising chemicals for the chemical industry. For example, it can be used for polymer synthesis, as a solvent, and a fuel additive. A number of publications about dimethyl carbonate (DMC) synthesis appeared recently [1–5]. Several synthetic routes affording DMC were reported; for example, methanolysis of phosgene [6], oxidative carbonylation of methanol [7], transesterification of ethylene carbonate [8] or urea [9], electrochemical synthesis [10], direct DMC synthesis from carbon dioxide and methanol [11]. Full accounts of the advantages and disadvantages of different synthesis methods can be found in [12–15]. The reaction of CO_2 and methanol to produce DMC deserves attention as it is one of promising routes that are based on green chemistry and sustainable development.

A difficulty of the direct DMC synthesis from CO_2 and methanol is the activation of highly stable CO_2 molecules. Various approaches were employed to increase DMC yield (methanol conversion times selectivity toward DMC), such as the application of supercritical CO_2, dehydrating agents, developing efficient catalysts [13–23]. Improved yield of DMC was continuously reported in many publications [24–27].

A fundamental way to increase DMC yield is to develop efficient catalysts to activate CO_2. A large number of catalysts were investigated for the conversion of CO_2 and methanol into DMC. Ikeda [28] reported that commercially available ZrO_2 modified with H_3PO_4 afforded a DMC yield of 0.42%. Tomishige [29] used a CeO_2-ZrO_2 catalyst, and the DMC yield reached 0.76%. Aresta [30] reported an Al_2O_3/CeO_2 catalyst with 0.45% DMC yield. Lee [31] synthesized a $5Ga_2O_3/Ce_{0.6}Zr_{0.4}O_2$ catalyst which afforded 0.47% yield of DMC. High DMC yields (>95%) can be achieved via the use of dehydrating agents [11,13,15,32]. Dehydrating agents are generally expensive and are difficult to recycle though. A relatively high yield (16%) was reported recently for the process in the presence of a titanium-based zeolitic thiophenebenzimidazolate framework only [33].

We had been studying the direct DMC synthesis by heterogeneous Cu-Ni catalysts in the absence of dehydrating compounds [34–42]. One catalyst type is Cu-Ni@VSiO (copper and nickel supported on V_2O_5/SiO_2 carrier). Copper and nickel are active components of the catalysts. The presence of "VO_n" species in catalyst may provide additional sites for reactant activation [34,43]. In the present study, a novel sulfuration method was employed to synthesize Cu-Ni@VSiO catalyst. When compared with a catalyst that was obtained by a traditional solution method, the structure and properties of the catalyst changed significantly. The activities of supported metal catalysts are usually determined by many factors, including metal dispersion, morphology of metal clusters, metal particle size, and metal-support interaction. The synthesized catalysts consisted of uniform particles without any agglomeration phenomenon. Accordingly, the novel sulfuration method solved many inevitable defects of the traditional synthetic method.

2. Results and Discussion

2.1. Chemical Structure and Morphology of Synthesized Catalysts

2.1.1. Characterization of Catalyst Support VSiO Microstructure

VSiO supports with close contents of vanadium and silicon were synthesized by the traditional solution and sulfuration methods, and their chemical structures were characterized by several techniques. Fourier transform infrared spectrum (FTIR) spectra of the supports are shown in Figure 1. Both the positions and relative intensities of peaks are obviously different. The following peak position shifts were observed: 3466 cm^{-1} moved to 3428 cm^{-1}, 1679 cm^{-1} moved to 1624 cm^{-1}, 1146 cm^{-1} moved to 1101 cm^{-1}, 867 cm^{-1} moved to 806 cm^{-1}. Signals from SiO_2 dominate in the IR spectra of the obtained materials [34,44–46].

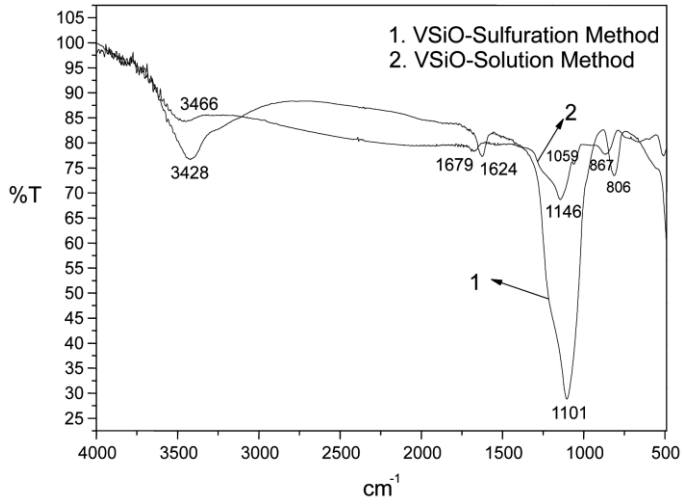

Figure 1. FTIR spectra of the VSiO supports: 1—sulfuration method; 2—solution method.

The X-ray diffraction (XRD) spectra in Figure 2 demonstrate the peaks of amorphous SiO_2 and the absence of peaks corresponding to crystalline phases, which may indicate that vanadium oxide species were well distributed over silica surface.

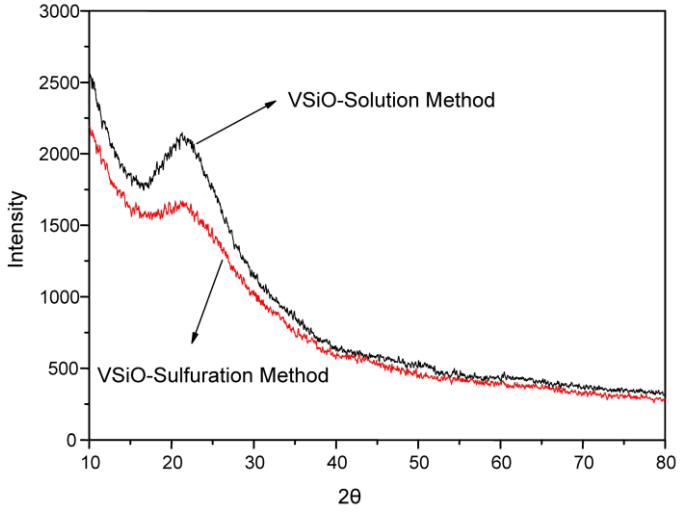

Figure 2. XRD profiles of the VSiO supports.

Temperature programmed reduction (TPR) technique was able to analyze the interaction between components of the supports. The reduction peak of VSiO obtained by the sulfuration method was observed at about 541 °C (Figure 3). In the case of VSiO synthesized by the solution method, two peaks appeared at about 554 °C and 605 °C. Therefore interaction mode between V_2O_5 and SiO_2 in the VSiO supports was significantly different, which led to different catalytic properties.

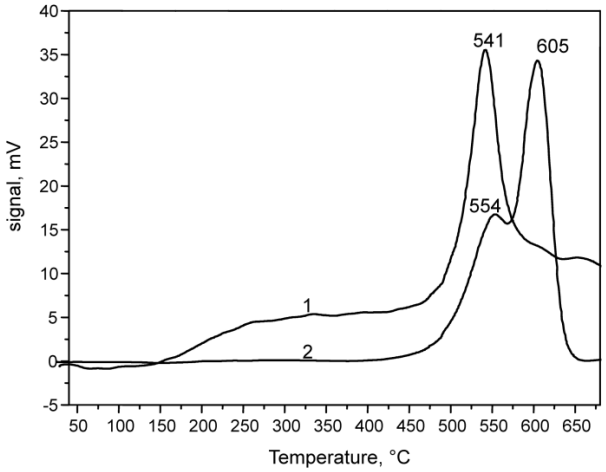

Figure 3. TPR profiles of the VSiO supports obtained by: 1—sulfuration method; 2—solution method.

In order to further analyze specific differences, the particle size and morphology for the different supports were estimated by Scanning electron microscopy (SEM) (Figure 4). VSiO obtained by the solution method consisted of larger particles and agglomeration phenomenon was obvious. In contrast, VSiO synthesized by the sulfuration method was composed of uniform small particles and agglomeration phenomenon was not observed. So, if the particle size and the morphology are considered, the sulfuration method is better than the solution method. Energy dispersive X-ray spectrometers (EDS) analysis was employed to make sure whether the proportion of elements in support was equal to the proportion used for synthesis (Figures 5 and 6). According to the experimental results, these two were nearly the same.

Consequently, the VSiO supports synthesized by the different synthetic methods with same synthetic ratio are very different according to FTIR, XRD, TPR, and SEM measuring techniques.

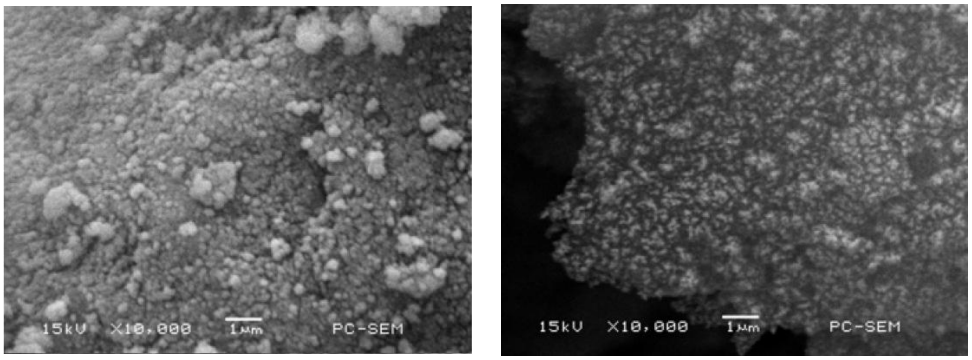

(**a**) (**b**)

Figure 4. SEM images of the VSiO supports obtained by: (**a**) Solution method; (**b**) Sulfuration method.

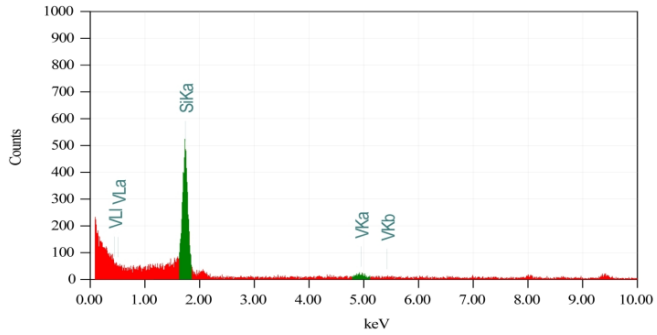

Element	Energy, keV	Mass, %	Atom, %
Si	1.739	89.72	94.1
V	4.949	10.28	5.94

Figure 5. Results of EDS analysis of the VSiO support obtained by the solution method.

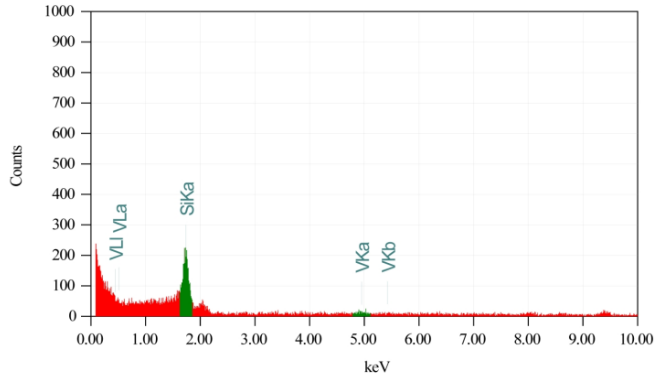

Element	Energy, keV	Mass, %	Atom, %
Si	1.739	88.71	93.4
V	4.949	11.29	6.56

Figure 6. Results of EDS analysis of the VSiO support obtained by the sulfuration method.

2.1.2. CuO-NiO@VSiO and Cu-Ni@VSiO Microstructure Characterization

CuO-NiO@VSiO (intermediate product of catalyst synthesis before reduction with H_2) and Cu-Ni@VSiO were synthesized by the traditional solution and novel sulfuration routes using the same synthetic ratio of reagents. Their microstructures were characterized by several techniques.

The following peaks were observed in XRD spectra (Figure 7): one peak of CuO(110) and one peak of CuNi alloy phase (111) in CuO-NiO@VSiO and Cu-Ni@VSiO that were obtained by the solution method, respectively; two peaks of CuO(110) and NiO(101), two peaks of CuNi alloy phase (111), (200) in CuO-NiO@VSiO and Cu-Ni@VSiO that were produced by the sulfuration method, respectively.

DMC synthesis from methanol and CO_2 is a heterogeneous catalytic reaction that is promoted by a catalyst crystalline phase. Therefore, more CuNi alloy phase is beneficial to improve catalytic efficiency.

TPR technique was employed to analyze the interaction between components of the catalysts (Figure 8). CuO reduction peak was at 263 °C and NiO reduction peak was at 418 °C for CuO-NiO@VSiO that was obtained by the sulfuration method [35]. In the case of CuO-NiO@VSiO synthesized by the solution method, these values were 302 °C and 424 °C, respectively. The lower reduction temperature for the CuO component in the first case (263 °C vs. 302 °C) is probably the consequence of weaker interaction of CuO with the support.

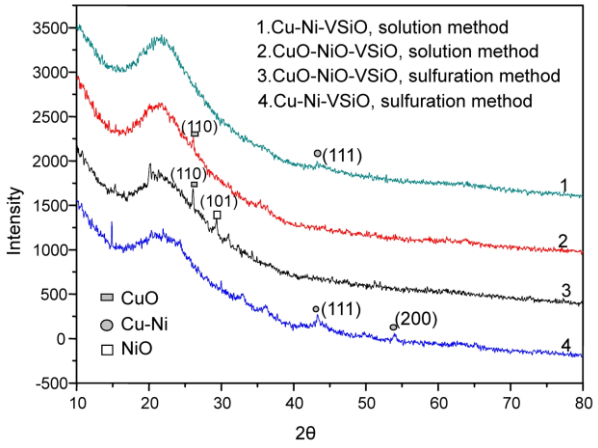

Figure 7. XRD patterns of Cu-Ni@VSiO and CuO-NiO@VSiO.

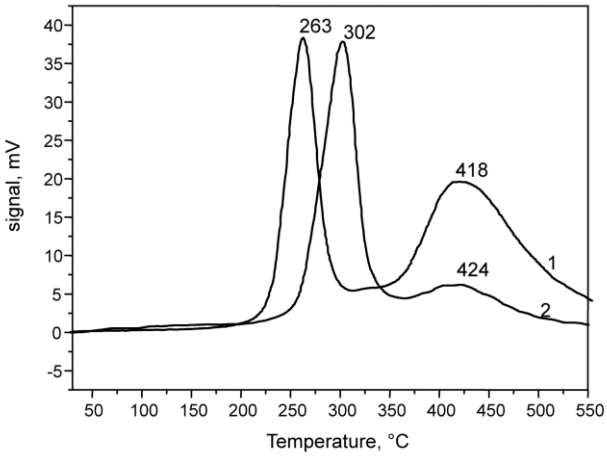

Figure 8. TPR profiles of CuO-NiO@VSiO obtained by: 1—sulfuration method, 2—solution method.

Temperature programmed desorption (CO_2-TPD) spectra revealed the characteristics of basic sites on the catalyst surface and the absorption capacity of CO_2 (Figure 9). The number of peaks represents the number of types of active centers and the area of a peak indicates the amount of active sites of

the catalyst. There was only one peak around 328 °C and 265 °C for Cu-Ni@VSiO obtained by the sulfuration and solution methods, respectively. Therefore, it was shown that only one type of active centers bonding CO_2 exists in each case. According to peak area values, the number of active centers for the catalyst that are produced by the sulfuration method is much higher than that for the catalyst produced by the solution method. Therefore, the adsorption strength of CO_2 and the activation extent of CO_2 for Cu-Ni@VSiO produced by the sulfuration method are higher when compared to those of Cu-Ni@VSiO synthesized by the solution method.

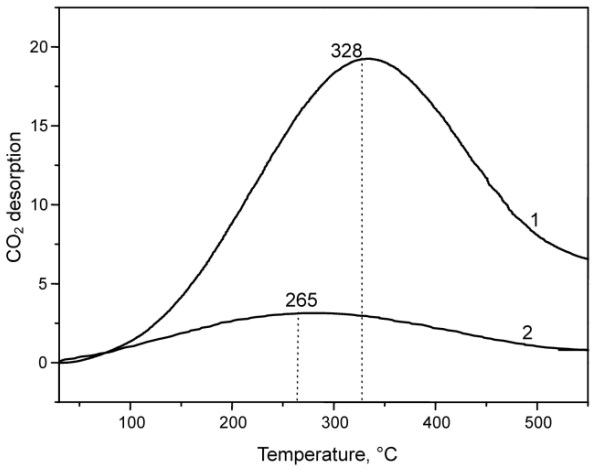

Figure 9. CO_2-TPD of Cu-Ni@VSiO obtained by: 1—sulfuration method, 2—solution method.

The NH_3-TPD (Figure 10) spectra revealed the characteristics of acid sites on catalyst surface and allowed to investigate the activation of methanol on catalyst. There is only one broad peak of NH_3 desorption, corresponding to one type of acid site, at around 294 °C and 140 °C, for Cu-Ni@VSiO that is produced by the sulfuration and solution methods, respectively. According to peak areas, much more acid sites were produced when catalyst support was synthesized via the sulfuration method. Consequently, the activation of methanol for this catalyst is expected to be stronger than for Cu-Ni@VSiO with support obtained by the solution method. The observed differences between the two catalysts in CO_2-TPD and NH_3-TPD profiles could be attributed to well-dispersed and smaller granular Cu-Ni particles on VSiO support in the case of Cu-Ni@VSiO with support that is synthesized by the sulfuration method, which provided extra acid and base sites.

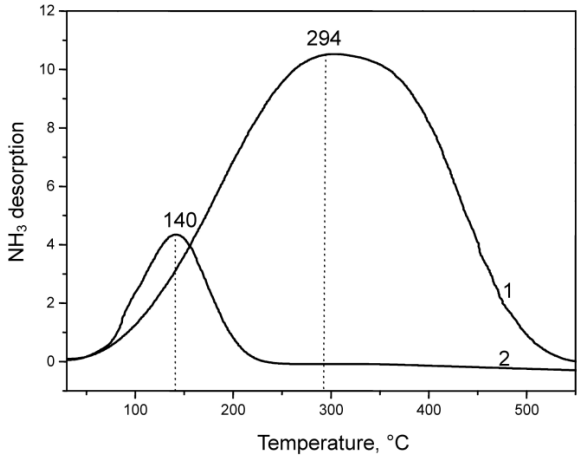

Figure 10. NH_3-TPD profiles of Cu-Ni@VSiO obtained by: 1—sulfuration method; 2—solution method.

In order to analyze the catalyst surface morphology, particle size, and composition, SEM and EDS analyses were employed. According to experimental results, Cu-Ni@VSiO surfaces were extremely different for the two synthesis methods (Figure 11). Cu-Ni@VSiO that was synthesized by the solution method consisted of larger particles and agglomeration phenomenon was observed in contrast to Cu-Ni@VSiO produced by the sulfuration method that was composed of uniform small particles without agglomeration. Based on the observation of the morphology, sulfuration synthesis method seems to be better when compared to the solution method. Additionally, EDS was measured to make sure whether actual element proportion in catalysts was the same as that used during catalyst synthesis (Figures 12 and 13). The experimental results proved that these two were close in values.

Consequently, CuO-NiO@VSiO and Cu-Ni@VSiO synthesized by the different synthetic methods with same synthetic ratio were extremely distinct according to XRD, TPR, CO_2-TPD, NH_3-TPD, SEM, and EDS measuring techniques.

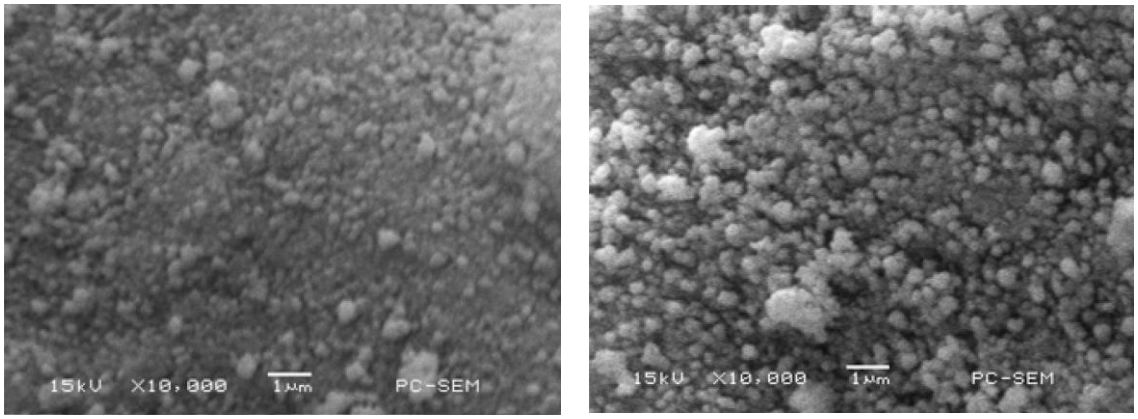

(**a**) (**b**)

Figure 11. SEM images of Cu-Ni@VSiO obtained by: (**a**) Solution method; and, (**b**) Sulfuration method.

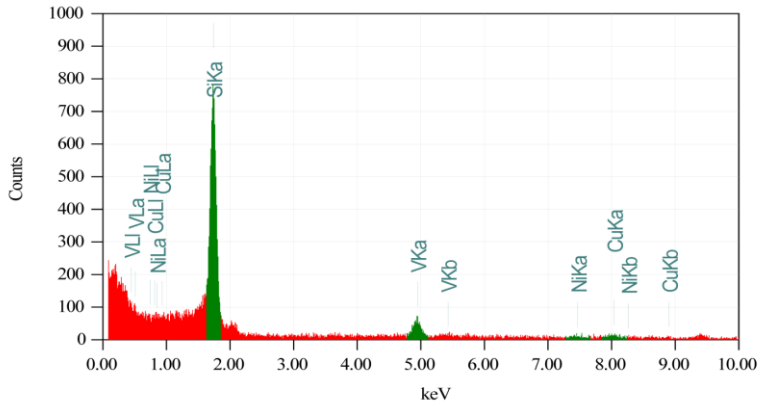

Element	Energy, keV	Mass, %	Atom, %
Cu	8.040	8.40	4.18
Ni	7.471	4.15	2.23
V	4.949	9.78	6.05
Si	1.739	77.7	87.5

Figure 12. Results of EDS analysis of Cu-Ni@VSiO obtained by the solution method.

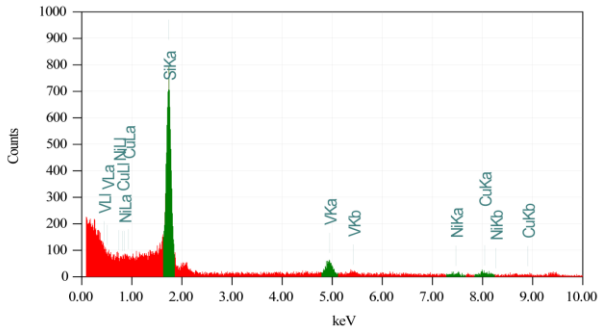

Element	Energy, keV	Mass, %	Atom, %
Cu	8.040	10.2	5.14
Ni	7.471	4.70	2.58
V	4.949	10.2	6.43
Si	1.739	74.9	85.8

Figure 13. Results of EDS analysis of Cu-Ni@VSiO obtained by the sulfuration method.

2.2. Catalytic Performance Characterization

The Cu-Ni@VSiO catalysts produced by the two different synthetic methods were evaluated in the reaction between methanol and CO_2 in a continuous tubular fixed-bed reactor. Different parameters (reaction temperature (T) and pressure (P), space velocity (SV), catalyst bulk density (D_B), CuO-NiO loading, and methanol bubbler temperature (T_{MB})) were varied in order to achieve optimal performance.

With the increase of reaction temperature, methanol conversion showed an increasing trend (Figure 14a). When the reaction temperature was increased beyond 140 °C, the methanol conversion decreased slightly. Generally, DMC selectivity decreased with the increase of reaction temperature. The kinetic energy of CO_2 and methanol molecules goes up with temperature and the probability of their interaction and of side reactions becomes higher, which could induce the increase of conversion and the decline of DMC selectivity. Elevated temperature also leads to lower concentration of the reactants in the reaction vessel. This may explain the reduction of methanol conversion at 160 °C.

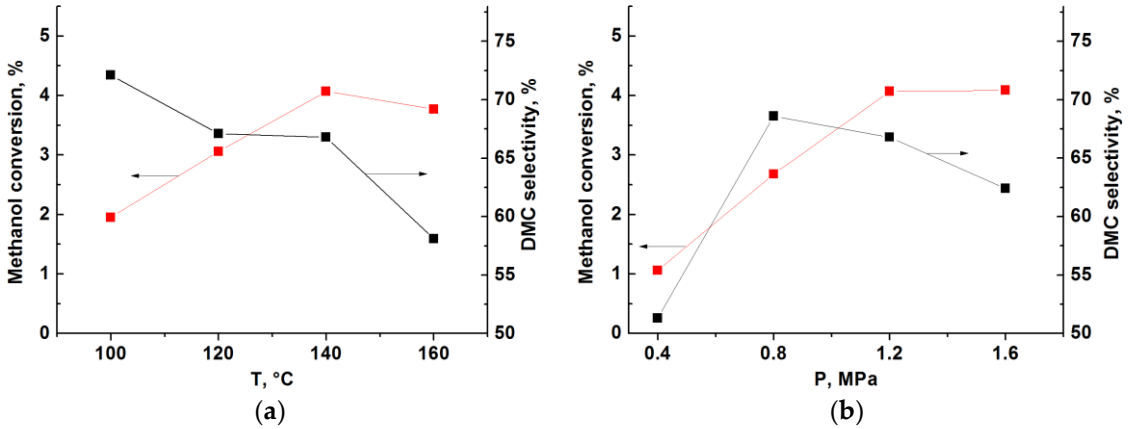

Figure 14. Effect of reaction temperature (**a**) and reaction pressure (**b**) on the performance of Cu-Ni@VSiO catalyst obtained by the sulfuration method.

The elevation of the reaction pressure favored higher methanol conversion, and the DMC selectivity went through a maximum (Figure 14b). For the reaction of DMC synthesis from CO_2 and methanol, the increased pressure is beneficial to shift the reaction equilibrium toward the products. Thus, the

equilibrium concentration of the target product increased correspondingly. A downward trend of DMC selectivity at P > 0.8 MPa could be a consequence of the increased rate of by-product formation.

With the increase of the space velocity, methanol conversion decreased, and DMC selectivity passed through a minimum (Figure 15a). As the space velocity increases, so does the amount of the reaction materials to be processed per unit time. If the catalyst does not have ability to process so many reactants, methanol conversion decreases. The trend of the DMC selectivity change is difficult to explain.

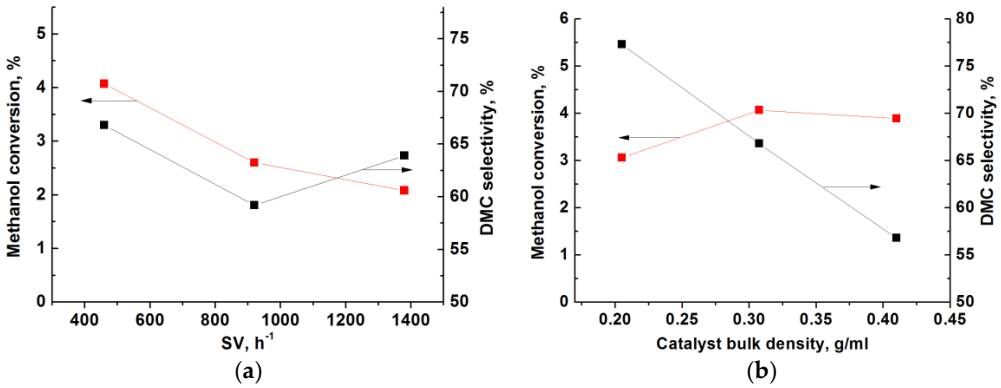

Figure 15. Effect of space velocity (**a**) and bulk density (**b**) on the performance of Cu-Ni@VSiO catalyst obtained by the sulfuration method.

Temperature, pressure, and space velocity exerted significant influence on catalyst performance. However, another important factor—catalyst bulk density—was found from a large number of experiments. Increasing the bulk density of the catalyst was helpful to improve methanol conversion, as follows from Figure 15b. If the bulk density of catalyst layer was too small, the reaction materials might pass through the catalyst where resistance was the least. Then, the catalyst layer could form an empty material inertia channel. As a result, the reaction materials could not contact well with the catalyst layer and then left it off. Increasing catalyst layer bulk density extended contact time between the reaction materials and the catalyst layer, which improved methanol conversion. Reasons for the drop of DMC selectivity upon raising the bulk density are not obvious.

The agglomeration of active components is one of problems for supported catalysts. Generally, the larger the load, the higher the extent of the agglomeration. Different amounts of active components are necessary for different supports to provide the best dispersion, least agglomeration, and, consequently, optimum catalytic performance. Within the limits that were studied by us, the higher was the active component load the lower was methanol conversion, and DMC selectivity went through a maximum (Figure 16a).

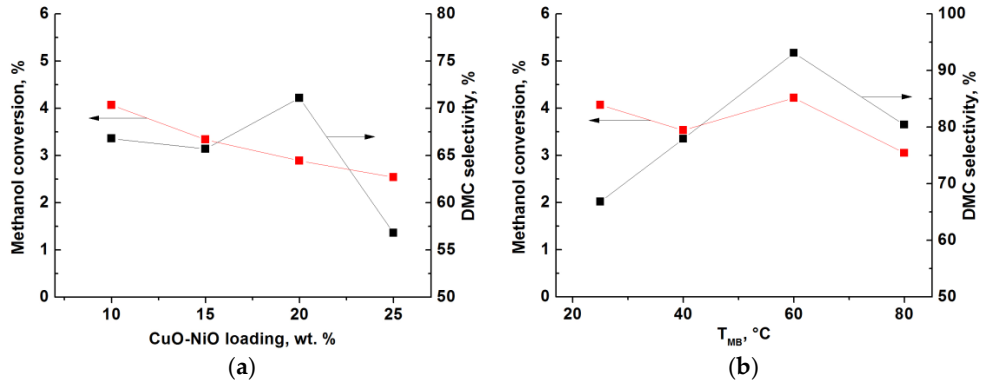

Figure 16. Effect of CuO-NiO loading (**a**) and methanol bubbler temperature (**b**) on the performance of Cu-Ni@VSiO catalyst obtained by the sulfuration method.

We also investigated the effect of methanol bubbler temperature on the reaction outcome. Methanol bubbler temperature can change the feed ratio of the reactants, that is, the molar ratio of CO_2 to methanol. Methanol conversion and DMC yield can be greatly improved by changing methanol bubbler temperature (Figure 16b). When the latter was 60 °C, optimum catalyst performance was observed.

The influence of temperature on the reaction was also studied for Cu-Ni@VSiO obtained by the solution method (Table 1). With the increase of reaction temperature, methanol conversion increased continuously and dimethyl carbonate (DMC) selectivity decreased. Table 2 lists data from the present work and other publications for different Cu-Ni catalysts tested in the direct DMC synthesis. Methanol conversion obtained in the presence of Cu-Ni@VSiO synthesized by the sulfuration method was 2.7 times higher than that of Cu-Ni@VSiO resulted from the solution method when they were tested under the same conditions. According to microstructure analysis, the novel catalytic material contained more Cu-Ni alloy phase and consisted of smaller particles. The TPD data showed the presence of higher amounts of centers interacting with CO_2 and methanol and higher strength of the interactions in this case. These differences in microstructure might be the reason of the more efficient catalytic performance.

Table 1. Effect of reaction temperature on the performance of Cu-Ni@VSiO catalyst obtained by the solution method.

Temperature, °C	Methanol Conversion, %	DMC Selectivity, %
100	0.47	96.3
120	0.84	91.5
140	1.69	86.3
160	1.73	80.6

Table 2. Comparison of the performance of different Cu-Ni catalysts.

Catalyst	T, °C	P, MPa	Reactor Type	MeOH Conversion, %	DMC Selectivity	Ref.
Cu-Ni@VSiO (sulfuration)	140	1.2	C [1]	4.2	93.1	present work
Cu-Ni@VSiO (solution)	140	1.2	C	1.7	86.3	present work
Cu-Ni@VSiO	140	0.1	C	14.5	87.8	[43]
Cu–Ni@ZIF-8 [2]	110	2	batch	12.8	50.0	[47]
Cu-Ni@VSiO [3]	120	0.1	C	4.0	85	[35]
Cu-Ni@VSiO	140	0.9	C	n.a.	87.1	[34]
Cu-Ni@SBA-15	110	1.2	continuous fixed-bed	ca 21	ca 20	[48]
Cu-Ni@TEG [2]	100	1.4	C	5.0	91.0	[36]
Cu-Ni@ KHNTs [2]	130	1.2	C	7.8	89.0	[37]
Cu-Ni@MS [2]	120	1.1	C	7.1	87	[38]
Cu-Ni@graphite	100	1.2	C	10.1	90.2	[40]
Cu-Ni-V@AC [2]	110	1.2	C	7.8	89.9	[41]
Cu-Ni@MWCNTs [2]	120	1.2	C	4.4	90.5	[42]

[1] Continuous tubular fixed bed reactor; [2] ZIF-8, TEG, KHNTs, MS, AC, MWCNTs are zeolitic imidazolate framework-8, thermally expanded graphite, K treated halloystite nanotubes, molecular sieves, activated carbon, multi-walled carbon nanotubes; [3] The reaction mixture was exposed to ultra violent (UV) radiation.

After comparison with the best data obtained previously, it can be concluded that Cu-Ni@VSiO catalyst synthesized by the sulfuration method affords the highest DMC selectivity coupled with a reasonable methanol conversion.

3. Materials and Methods

3.1. Catalyst Synthesis

3.1.1. Traditional Solution Synthetic Method of Cu-Ni@VSiO

Firstly, V_2O_5 was treated with excess hydrochloric acid at 90 °C, and the remaining hydrochloric acid was removed after reaction. Then nano-SiO_2 aqueous solution was added and the mixture was mechanically stirred for 30 min. After 12 h of aging, the liquid part was removed by decompressive rotary evaporation. The residue was dried at 120 °C for 24 h. The completely dried solid was ground with an agate mortar and passed through a 200 mesh sieve. Subsequently, the product was calcined in air at 450 °C for 5 h using a muffle furnace to get the VSiO support. Then, the product was mixed with ammonium solutions of metal nitrates (Cu:Ni mole ratio is 2:1) by equal volume impregnation. The resulting bimetallic/VSiO slurry was dried under reduced pressure in a rotary evaporator, and the obtained solid was further dried at 120 °C and calcined at 550 °C for 6 h to get a catalyst precursor. Subsequently, the latter was reduced in a stream of H_2 at 500 °C for 6 h to get the final Cu-Ni@VSiO catalyst.

3.1.2. Novel Sulfuration Method to Synthesize Cu-Ni@VSiO

Sulfur powder was reacted with $VOCl_3$ at 130 °C for 2 h in a round bottom flask to get $VOCl_2$. Then, $VOCl_2$ was dissolved in dimethylacetamide and nano-SiO_2 was added. The slurry was stirred at 90 °C for 12 h and was evaporated under reduced pressure in a rotary evaporator. The obtained solid was further dried under vacuum. The resulting substance was ground with an agate mortar and passed through a 200 mesh sieve. Subsequently, the product was calcined in air at 450 °C for 6 h to get the VSiO support. The same method, as described above, was used to load the Cu Ni bimetallic components to produce the final Cu-Ni@VSiO catalyst.

3.2. Catalysts Characterization

The X-ray powder diffraction was performed on Rigaku Dmax 2200 diffractometer (Rigaku Company, Tokyo, Japan) with graphite monochromatized Cu Kα radiation (λ = 0.154178 nm) at 40 kV and 30 mA. The sample was scanned from 10° to 80°, at a rate of 4°/min.

FTIR spectra were acquired on an Analect RFX-65A instrument (Analect Company, New York, NY, USA). TPD and TPR were implemented on a Quantachrom Chem-BET 3000 apparatus (Quantachrome Company, Boynton Beach, FL, USA) to determine the surface acid-base properties of catalysts.

SEM was performed on a Hitachi S-4800 system (Hitachi Company, Tokyo, Japan) that was equipped with an energy dispersive X-ray detector at 10.0 kV under high vacuum. The energy dispersion spectra were also recorded.

3.3. Evaluation of Catalytic Performance

The synthesis of DMC from methanol and CO_2 was carried out in a continuous tubular fixed-bed micro-reactor (Golden Eagle Technology Ltd., Tianjin, China). A detailed description of the reactor setup and data treatment was published previously [35,36,40]. CO_2 was purged into methanol container to get CO_2/methanol mixed gas. The mixed gas was then charged into the reactor (reactor internal diameter D = 10 mm, catalyst filling length L = 50 mm). Unless otherwise stated, the following parameters were used to carry out the reaction: T = 140 °C, P = 1.2 MPa, SV = 460 h^{-1}, D_B = 0.308 g/mL, T_{MB} = 25 °C, CuO-NiO loading 10 wt. %). The resulting products of the reaction were analyzed by a GC-7890F chromatograph (Techcomp Ltd., Shanghai, China) equipped with a flame ionization detector. Samples were introduced through a six-way valve that was connected to the reactor.

4. Conclusions

In summary, the use of the VSiO support synthesized by the novel sulfuration method afforded a more efficient Cu-Ni catalyst compared to the catalyst with the support that was obtained by the solution method. The former one contained more Cu-Ni phase and interacted with CO_2 and methanol stronger that the latter. The novel synthetic method extremely changed catalyst microstructure and the catalytic performance was greatly improved. Catalytic activity of Cu-Ni@VSiO that was obtained by the sulfuration method was about three times higher than that of Cu-Ni@VSiO produced by the solution method. For the studied direct DMC synthesis from methanol and CO_2, the optimal reaction conditions were found to have the following values: T = 140 °C, P = 1.2 MPa, SV = 460 h^{-1}, D_B = 0.308 g/mL, T_{MB} = 60 °C, and metal oxides loading 10 wt. %.

Acknowledgments: The authors would like to thank the National Natural Science Foundation of China (Grant No. 21376276, 21643002), the Guangdong Province Sci & Tech Bureau (Key Strategic Project Grant No. 2008A080800024, 10151027501000096), and Chinese Universities Basic Research Founding (171gjc37) for financial support of the work.

Author Contributions: Min Xiao and Shuanjin Wang conceived and designed the experiments; Meng Zhang performed the experiments; Kirill A. Alferov and Dongmei Han analyzed the data; Yuezhong Meng wrote the paper.

Conflicts of Interest: The authors declare no conflict of interest.

References

1. Marin, C.M.; Li, L.; Bhalkikar, A.; Doyle, J.E.; Zeng, X.C.; Cheung, C.L. Kinetic and mechanistic investigations of the direct synthesis of dimethyl carbonate from carbon dioxide over ceria nanorod catalysts. *J. Catal.* **2016**, *340*, 295–301. [CrossRef]
2. Stoian, D.; Bansode, A.; Medina, F.; Urakawa, A. Catalysis under microscope: Unraveling the mechanism of catalyst de- and re-activation in the continuous dimethyl carbonate synthesis from CO_2 and methanol in the presence of a dehydrating agent. *Catal. Today* **2017**, *283*, 2–10. [CrossRef]
3. Ghorbel, S.B.; Medina, F.; Ghorbel, A.; Segarra, A.M. Phosphoric acid intercalated Mg–Al hydrotalcite-like compounds for catalytic carboxylation reaction of methanol in a continuous system. *Appl. Catal. A Gen.* **2015**, *493*, 142–148. [CrossRef]
4. Zhang, M.; Xiao, M.; Wang, S.J.; Han, D.M.; Lu, Y.X.; Meng, Y.Z. Cerium oxide-based catalysts made by template-precipitation for the dimethyl carbonate synthesis from Carbon dioxide and methanol. *J. Clean. Prod.* **2015**, *103*, 847–853. [CrossRef]
5. Yang, Z.-Z.; Zhao, Y.-N.; He, L.-N.; Gao, J.; Yin, Z.-S. Highly efficient conversion of carbon dioxide catalyzed by polyethylene glycol-functionalized basic ionic liquids. *Green Chem.* **2012**, *14*, 519–527. [CrossRef]
6. Drake, N.L.; Carter, R.M. Some representative carbonates and carbo-ethoxy derivatives related to ethylene glycol[1]. *J. Am. Chem. Soc.* **1930**, *52*, 3720–3724. [CrossRef]
7. Curnutt, G.L. Catalytic Vapor Phase Process for Producing Dihydrocarbyl Carbonates. U.S. Patent 5,004,827, 2 April 1991.
8. Feng, X.-J.; Lu, X.-B.; He, R. Tertiary amino group covalently bonded to MCM-41 silica as heterogeneous catalyst for the continuous synthesis of dimethyl carbonate from methanol and ethylene carbonate. *Appl. Catal. A Gen.* **2004**, *272*, 347–352. [CrossRef]
9. Aresta, M. Perspectives in the use of carbon dioxide. *Quim. Nova* **1999**, *22*, 269–272. [CrossRef]
10. Yamanaka, I.; Funakawa, A.; Otsuka, K. Electrocatalytic synthesis of DMC over the Pd/VGCF membrane anode by gas–liquid–solid phase-boundary electrolysis. *J. Catal.* **2004**, *221*, 110–118. [CrossRef]
11. Bansode, A.; Urakawa, A. Continuous DMC Synthesis from CO_2 and Methanol over a CeO_2 Catalyst in a Fixed Bed Reactor in the Presence of a Dehydrating Agent. *ACS Catal.* **2014**, *4*, 3877–3880. [CrossRef]
12. Tamboli, A.H.; Chaugule, A.A.; Kim, H. Catalytic developments in the direct dimethyl carbonate synthesis from carbon dioxide and methanol. *Chem. Eng. J.* **2017**, *323*, 530–544. [CrossRef]
13. Santos, B.A.V.; Silva, V.M.T.M.; Loureiro, J.M.; Rodrigues, A.E. Review for the Direct Synthesis of Dimethyl Carbonate. *ChemBioEng Rev.* **2014**, *1*, 214–229. [CrossRef]

14. Sakakura, T.; Kohno, K. The synthesis of organic carbonates from carbon dioxide. *Chem. Commun.* **2009**, 1312–1330. [CrossRef] [PubMed]
15. Fu, Z.; Meng, Y. Research Progress in the Phosgene-Free and Direct Synthesis of Dimethyl Carbonate from CO_2 and Methanol. In *Chemistry beyond Chlorine*; Tundo, P., He, L.-N., Lokteva, E., Mota, C., Eds.; Springer International Publishing: Cham, Switzerland, 2016; pp. 363–385. ISBN 978-3-319-30071-9.
16. Cao, Y.; Cheng, H.; Ma, L.; Liu, F.; Liu, Z. Research Progress in the Direct Synthesis of Dimethyl Carbonate from CO_2 and Methanol. *Catal. Surv. Asia* **2012**, *16*, 138–147. [CrossRef]
17. Zhou, Y.J.; Wang, S.J.; Xiao, M.; Han, D.M.; Lu, Y.X.; Meng, Y.Z. Novel Cu-Fe bimetal catalyst for the formation of dimethyl carbonate from carbon dioxide and methanol. *RSC Adv.* **2012**, *17*, 6831–6837. [CrossRef]
18. Choi, J.C.; He, L.N.; Yasuda, H.; Sakakura, T. Selective and high yield synthesis of dimethyl carbonate directly from carbon dioxide and methanol. *Green Chem.* **2002**, 230–234. [CrossRef]
19. Fang, S.N.; Fujimoto, K. Direct synthesis of dimethyl carbonate from carbon dioxide and methanol catalyzed by base. *Appl. Catal. A Gen.* **1996**, *142*, L1–L3. [CrossRef]
20. Kumar, P.; With, P.; Srivastava, V.C.; Glaser, R.; Mishra, I.M. Conversion of carbon dioxide along with methanol to dimethyl carbonate over ceria catalyst. *J. Environ. Chem. Eng.* **2015**, *3*, 2943–2947. [CrossRef]
21. Tamboli, A.H.; Chaugule, A.A.; Kim, H. Highly selective and multifunctional chitosan/ionic liquids catalyst for conversion of CO_2 and methanol to dimethyl carbonates at mild reaction conditions. *Fuel* **2016**, *166*, 495–501. [CrossRef]
22. Saada, R.; Kellici, S.; Heil, T.; Morgan, D.; Saha, B. Greener synthesis of dimethyl carbonate using a novel ceria-zirconia oxide/graphene nanocomposite catalyst. *Appl. Catal. B Environ.* **2015**, *168*, 353–362. [CrossRef]
23. Kumar, S.; Kumar, P.; Jain, S.L. Graphene oxide immobilized copper phthalocyanine tetrasulphonamide: The first heterogenized homogeneous catalyst for dimethylcarbonate synthesis from CO_2 and methanol. *J. Mater. Chem. A* **2014**, 18861–18866. [CrossRef]
24. Eta, V.; Maki-Arvela, P.; Leino, A.R.; Kordas, K.; Salmi, T.; Murzin, D.Y.; Mikkola, J.P. Synthesis of Dimethyl Carbonate from Methanol and Carbon Dioxide: Circumventing Thermodynamic Limitations. *Ind. Eng. Chem. Res.* **2010**, *49*, 9609–9617. [CrossRef]
25. Fan, B.B.; Li, H.Y.; Fan, W.B.; Zhang, J.L.; Li, R.F. Organotin compounds immobilized on mesoporous silicas as heterogeneous catalysts for direct synthesis of dimethyl carbonate from methanol and carbon dioxide. *Appl. Catal. A Gen.* **2010**, *372*, 94–102. [CrossRef]
26. Kohno, K.; Choi, J.C.; Ohshima, Y.; Yasuda, H.; Sakakura, T. Synthesis of dimethyl carbonate from carbon dioxide catalyzed by titanium alkoxides with polyether-type ligands. *ChemSusChem* **2008**, *1*, 186–188. [CrossRef] [PubMed]
27. Wu, X.L.; Shu, D.; Meng, Y.Z. Direct synthesis of dimethyl carbonate from CO_2 and methanol. *Res. J. Chem. Environ.* **2005**, *9*, 74–79. [CrossRef]
28. Ikeda, Y.; Sakaihori, T.; Tomishige, K.; Fujimoto, K. Promoting effect of phosphoric acid on zirconia catalysts in selective synthesis of dimethyl carbonate from methanol and carbon dioxide. *Catal. Lett.* **2000**, *66*, 59–62. [CrossRef]
29. Tomishige, K.; Kunimori, K. Catalytic and direct synthesis of dimethyl carbonate starting from carbon dioxide using CeO_2-ZrO_2 solid solution heterogeneous catalyst: Effect of H_2O removal from the reaction system. *Appl. Catal. A Gen.* **2002**, *237*, 103–109. [CrossRef]
30. Aresta, M.; Dibenedetto, A.; Pastore, C.; Cuocci, C.; Aresta, B.; Cometa, S.; De Giglio, E. Cerium(IV)oxide modification by inclusion of a hetero-atom: A strategy for producing efficient and robust nano-catalysts for methanol carboxylation. *Catal. Today* **2008**, *137*, 125–131. [CrossRef]
31. Lee, H.J.; Park, S.; Song, I.K.; Jung, J.C. Direct Synthesis of Dimethyl Carbonate from Methanol and Carbon Dioxide over $Ga_2O_3/Ce_{0.6}Zr_{0.4}O_2$ Catalysts: Effect of Acidity and Basicity of the Catalysts. *Catal. Lett.* **2011**, *141*, 531–537. [CrossRef]
32. Zhao, T.; Hu, X.; Wu, D.; Li, R.; Yang, G.; Wu, Y. Direct synthesis of dimethyl carbonate from CO_2 and methanol at room temperature using imidazolium hydrogen carbonate ionic liquid as recyclable catalyst and dehydrant. *ChemSusChem* **2017**, *10*, 2046–2052. [CrossRef] [PubMed]
33. Verma, S.; Nasir Baig, R.B.; Nadagouda, M.N.; Varma, R.S. Fixation of carbon dioxide into dimethyl carbonate over titanium-based zeolitic thiophenebenzimidazolate framework. *Sci. Rep.* **2017**, *7*, 655. [CrossRef] [PubMed]

34. Wu, X.L.; Meng, Y.Z.; Xiao, M.; Lu, Y.X. Direct synthesis of dimethyl carbonate (DMC) using Cu-Ni/VSO as catalyst. *J. Mol. Catal. A Chem.* **2006**, *249*, 93–97. [CrossRef]
35. Wang, X.J.; Xiao, M.; Wang, S.J.; Lu, Y.X.; Meng, Y.Z. Direct synthesis of dimethyl carbonate from carbon dioxide and methanol using supported copper (Ni, V, O) catalyst with photo-assistance. *J. Mol. Catal. A Chem.* **2007**, *278*, 92–96. [CrossRef]
36. Bian, J.; Xiao, M.; Wang, S.J.; Lu, Y.X.; Meng, Y.Z. Novel application of thermally expanded graphite as the support of catalysts for direct synthesis of DMC from CH_3OH and CO_2. *J. Colloid Interface Sci.* **2009**, *334*, 50–57. [CrossRef] [PubMed]
37. Zhou, Y.; Wang, S.; Xiao, M.; Han, D.; Lu, Y.; Meng, Y. Formation of dimethyl carbonate on nature clay supported bimetallic copper-nickel catalysts. *J. Clean. Prod.* **2015**, *103*, 925–933. [CrossRef]
38. Chen, H.; Wang, S.; Xiao, M.; Han, D.; Lu, Y.; Meng, Y. Direct synthesis of dimethyl carbonate from CO_2 and CH_3OH using 0.4 nm molecular sieve supported Cu-Ni bimetal catalyst. *Chin. J. Chem. Eng.* **2012**, *20*, 906–913. [CrossRef]
39. Bian, J.; Xiao, M.; Wang, S.J.; Lu, Y.X.; Meng, Y.Z. Highly effective direct synthesis of DMC from CH_3OH and CO_2 using novel Cu-Ni/C bimetallic composite catalysts. *Chin. Chem. Lett.* **2009**, *20*, 352–355. [CrossRef]
40. Bian, J.; Xiao, M.; Wang, S.; Wang, X.; Lu, Y.; Meng, Y. Highly effective synthesis of dimethyl carbonate from methanol and carbon dioxide using a novel copper-nickel/graphite bimetallic nanocomposite catalyst. *Chem. Eng. J.* **2009**, *147*, 287–296. [CrossRef]
41. Bian, J.; Xiao, M.; Wang, S.; Lu, Y.; Meng, Y. Direct synthesis of DMC from CH_3OH and CO_2 over V-doped Cu-Ni/AC catalysts. *Catal. Commun.* **2009**, *10*, 1142–1145. [CrossRef]
42. Bian, J.; Xiao, M.; Wang, S.J.; Lu, Y.X.; Meng, Y.Z. Carbon nanotubes supported Cu-Ni bimetallic catalysts and their properties for the direct synthesis of dimethyl carbonate from methanol and carbon dioxide. *Appl. Surf. Sci.* **2009**, *255*, 7188–7196. [CrossRef]
43. Zhong, S.H.; Wang, J.W.; Xiao, X.F.; Li, H.S. Dimethyl carbonate synthesis from carbon dioxide and methanol over Cu-Ni/MoSiO(VSiO) catalysts. In *12th International Congress on Catalysis*; Corma, A., Melo, F.V., Mendioroz, S., Fierro, J.L.G., Eds.; Studies in Surface Science and Catalysis; Elsevier: Amsterdam, The Netherlands, 2000; Volume 130, pp. 1565–1570.
44. Wang, D.; Zhou, L.; Feng, X.; Zhao, N.; Yang, B. Polysilicic acid gel method derived V_2O_5/SiO_2 composite materials: Synthesis and characterization. *AIP Conf. Proc.* **2017**, *1794*, 020021. [CrossRef]
45. Khatab, T.K.; Abdelghany, A.M.; Soliman, H.A. V_2O_5/SiO_2 as a Heterogeneous Catalyst in the Synthesis of bis(indolyl)methanes under Solvent Free Condition. *Silicon* **2017**, 1–6. [CrossRef]
46. Musić, S.; Filipović-Vinceković, N.; Sekovanić, L. Precipitation of amorphous SiO_2 particules and their properties. *Braz. J. Chem. Eng.* **2011**, *28*, 89–94. [CrossRef]
47. Poungsombate, A.; Imyen, T.; Dittanet, P.; Embley, B.; Kongkachuichay, P. Direct synthesis of dimethyl carbonate from CO_2 and methanol by supported bimetallic Cu–Ni/ZIF-8 MOF catalysts. *J. Taiwan Inst. Chem. Eng.* **2017**, *80*, 16–24. [CrossRef]
48. Pimprom, S.; Sriboonkham, K.; Dittanet, P.; Föttinger, K.; Rupprechter, G.; Kongkachuichay, P. Synthesis of copper-nickel/SBA-15 from rice husk ash catalyst for dimethyl carbonate production from methanol and carbon dioxide. *J. Ind. Eng. Chem.* **2015**, *31*, 156–166. [CrossRef]